THE JOURNAL OF BIOLOGICAL CHEMISTRY VOL. 287, NO. 12, pp. 9534–9546, March 16, 2012

Mitochondrial 3β-Hydroxysteroid Dehydrogenase Enzyme Activity Requires Reversible pH-dependent Conformational Change at the Intermembrane Space*[S]

Received for publication, December 12, 2011, and in revised form, January 16, 2012 Published, JBC Papers in Press, January 19, 2012, DOI 10.1074/jbc.M111.333278

Manoj Prasad[‡], James L. Thomas[§], Randy M. Whittal[¶], and Himangshu S. Bose[‡‖1]

From the [‡]Mercer University School of Medicine and [‖]Memorial University Medical Center, Savannah, Georgia 31404, the [§]Division of Basic Medical Sciences, Mercer University School of Medicine, Macon, Georgia 31207, and the [¶]Department of Chemistry, University of Alberta, Edmonton, Alberta T6G 2G2, Canada

Background: Mitochondrial intermembrane proton gradient is essential for dual functionality of 3β-hydroxysteroid dehydrogenase 2 (3βHSD2) enzyme.
Results: 3βHSD2 is more active in a partially unfolded conformation.
Conclusion: Reversible conformation of 3βHSD2 is a mandatory requirement for the biological activity at the intermembrane space.
Significance: Mitochondrial proton gradient activates 3βHSD2 in a molten globule conformation.

The inner mitochondrial membrane protein 3β-hydroxysteroid dehydrogenase 2 (3βHSD2) synthesizes progesterone and androstenedione through its dehydrogenase and isomerase activities. This bifunctionality requires 3βHSD2 to undergo a conformational change. Given its proximity to the proton pump, we hypothesized that pH influences 3βHSD2 conformation and thus activity. Circular dichroism (CD) showed that between pH 7.4 and 4.5, 3βHSD2 retained its primarily α-helical character with a decrease in α-helical content at lower pH values, whereas the β-sheet content remained unchanged throughout. Titrating the pH back to 7.4 restored the original conformation within 25 min. Metabolic conversion assays indicated peak 3βHSD2 activity at pH 4.5 with ~2-fold more progesterone synthesized at pH 4.5 than at pH 3.5 and 7.4. Increasing the 3βHSD2 concentration from 1 to 40 μg resulted in a 7-fold increase in progesterone at pH 4.5, but no change at pH 7.4. Incubation with guanidinum hydrochloride (GdmHCl) showed a three-step cooperative unfolding of 3βHSD2 from pH 7.4 to 4.5, possibly due to the native state unfolding to the intermediate ion core state. With further decreases in pH, increasing concentrations of GdmHCl led to rapid two-step unfolding that may represent complete loss of structure. Between pH 4 and 5, the two intermediate states appeared stable. Stopped-flow kinetics showed slower unfolding at around pH 4, where the protein is in a pseudostable state. Based on our data, we conclude that at pH 4–5, 3βHSD2 takes on a molten globule conformation that promotes the dual functionality of the enzyme.

Human 3β-hydroxysteroid dehydrogenase (3βHSD)[2] plays a central role in the synthesis of several steroid hormones and is thus essential for the survival of all species. Steroidogenic tissues do not store steroids, so synthesis occurs in the mitochondria on an as needed basis. Enzymes involved in the steroidogenic pathway are present in all steroidogenic tissues and some nonsteroidogenic tissues, including kidney and skin. 3βHSD is encoded by two distinct genes and expressed in a tissue-specific pattern (1, 2), with 3βHSD2 expressed exclusively in the adrenal gland, ovary, and testes. 3βHSD2, which lacks a heme group and requires NAD^+ as a cofactor for activity, catalyzes the conversion of multiple steroids in the pathway: pregnenolone to progesterone, 17α-hydroxypregnenolone to 17α-hydroxyprogesterone, and dehydroepiandrosterone to androstenedione (4-androstene-3,17-dione). Synthesis of these steroids requires that 3βHSD2 functions as both a dehydrogenase and isomerase, which it does as a single polypeptide.

The compartment-specific location of 3βHSD2 in the mitochondria had remained elusive since the time of its discovery; however, we recently reported that the protein localizes to the inter membrane space (IMS) without insertion into the inner mitochondrial membrane (IMM) (3). Specifically, we demonstrated that 3βHSD2 associates with several translocase complex proteins in the mitochondria. Translocase complexes, responsible for the import and sorting of mitochondrial proteins, can be found at either the outer mitochondrial membrane (OMM) or the IMM. We discovered that 3βHSD2 associates closely with the IMM protein Tim50, allowing further and transient associations with Tim23, and Tom22 (3), an OMM protein whose C terminus faces the IMS (3). 3βHSD2 has to adopt a flexible conformation to coordinate the continuous interaction with these proteins. Any change in the arrangement of the 3βHSD2 stoichiometry with Tim50, Tim23, or Tom22 ablates steroidogenesis (3).

Most matrix proteins carry a positively charged N-terminal presequence that is proteolytically removed after import. After

* This work was supported, in whole or in part, by National Institutes of Health Grant HD057876 (to H. S. B.), the Anderson Cancer Institute, and the Mercer University School of Medicine.
[S] This article contains supplemental Figs. S1 and S2.
[1] To whom correspondence should be addressed: Hoskins Research Bldg., 4700 Waters Ave., Savannah, GA 31404. Tel.: 912-350-1710; Fax: 912-350-1765; E-mail: bose_hs@mercer.edu or bosehi1@memorialhealth.com.
[2] The abbreviations used are: 3βHSD2, 3β-hydroxysteroid dehydrogenase 2; ANS, 8-anilino-1-naphthalenesulfonic acid; IMS, intermembrane space; IMS, inner mitochondrial membrane; CMC, critical micelle concentration; GdmHCl, guanidinum hydrochloride; OMM, outer mitochondrial membrane; VDAC, voltage-dependent anion channel; RT, retention time; Tm, temperature.

translocations through the TOM complex at the OMM, the preproteins are directed to the membrane potential ($\Delta\Psi$)-driven presequence translocase of the IMM (4, 5). Some inner membrane proteins carry a hydrophobic sorting sequence behind the cleavable matrix-targeting signal and thus arrested in the IMM (6). After passing through the TOM channel, precursors do not engage the presequence translocase, but use separate machinery for transport to and insertion into the IMM.

In vitro, most proteins spontaneously fold into a unique, thermodynamically stable, three-dimensional conformation. Although the physical-chemical principles of folding processes are not fully understood, theoretical studies have shown that the free energy landscapes for protein folding are most often biased like a funnel toward the structurally well defined native state (7–10). This implies that the transition state structure within a given folding resembles the native state of the protein. Mitochondrial specific proteins that undergo membrane insertion form "molten-disc" intermediates that have a partial secondary structure with the β-strands sitting flat on the membrane surface (11). The fact that we observed a correlation between 3βHSD2 activity and association with components of the inner and outer mitochondrial translocases strongly suggests that 3βHSD2 undergoes a conformational change during catalysis. Moreover, protein conformation and folding are often sensitive to pH. With decreasing pH, most native proteins first lose tertiary and then secondary structure, so that under strongly acidic conditions, they revert to an unstructured random coil. As an inner mitochondrial resident protein (12), 3βHSD2 faces the proton gradient generated by the proton pump and thus may undergo the conformational change required for its function. Because 3βHSD2 is not integrated into the IMM, it likely faces a continuous change in proton gradient, which may result in an equilibrium of transient conformational changes that can be described as a molten globule state. Using different biochemical and biophysical tools, here we show that the two different functional activities of 3βHSD2 at the inner mitochondrial membrane is possible due to a partially open conformation and remains in equilibrium at two different states with a minor change in free energy (ΔG).

EXPERIMENTAL PROCEDURES

Expression, Purification, and Characterization of 3βHSD2 Protein—3βHSD2 was expressed as a recombinant protein in the baculovirus system (13, 14). Briefly, recombinant baculovirus containing 3βHSD2 cDNA was added to 1.5×10^9 Sf9 cells (1 liter) at a multiplicity of infection of 10. To identify recombinant 3βHSD2, proteins from Sf9 cells were separated by SDS-polyacrylamide (12%) gel electrophoresis, probed with our anti-3βHSD2 polyclonal antibody, and detected using the West Pico Western blotting system (Pierce). The enzyme was purified from the 100,000 × *g* pellet of Sf9 cells (13, 14) in the presence of the low-critical micelle concentration (CMC) detergent, Igepal CO 720 (Rhodia, Inc., Cranbury, NJ), which is necessary to elute the enzyme from the DEAE-ion exchange column (13, 14). Using hydroxyapatite chromatography, we replaced Igepal with Cymal-5 (Anatrace, Inc., Maumee, OH), an UV invisible high-CMC detergent. The 3βHSD2 fraction pool from the DEAE column was applied to the hydroxyapatite column (1 mg of protein/ml of packed gel); washed with 3.5 column volumes of 0.025 M potassium phosphate, pH 7.5, 20% glycerol, 0.1 mM EDTA, 0.01 M NAD, 1.8 mM Cymal-5, and eluted with 0.30 M potassium phosphate, pH 7.5, 20% glycerol, 0.1 mM EDTA, 0.01 M NAD, 1.8 mM Cymal-5. The peak of 3βHSD2 activity was pooled and found to be free of Igepal CO-720 based on absorbance at 280 nm. Protein concentrations were determined by the guanidinum hydrochloride denaturation method (15) to avoid errors in extinction coefficients, but the total mitochondrial protein was estimated by (Bio-Rad dye reagents, Hercules, CA) using bovine serum albumin as the standard. During enzyme purification, the isomerase activity of 3βHSD2 was measured by the initial absorbance increase at 241 nm (due to 4-androstene-3,17-dione, androstenedione formation from the intermediate substrate, 5-androstene-3,17-dione) as a function of time. Blank assays (zero-enzyme, zero-substrate) assured that specific isomerase activity was measured as opposed to nonenzymatic, "spontaneous" isomerization (13). Changes in absorbance were measured with a Varian (Sugar Land, TX) Cary 300 recording spectrophotometer.

Anti-3βHSD2 Antiserum—We raised antiserum against recombinant, wild-type 3βHSD2 protein expressed in baculovirus. Purified 3βHSD2 protein was dissolved in Freund's adjuvant and 0.2 mg was injected into each of 2 New Zealand White rabbits, followed by a booster injection 6 weeks later (Lampire Biologicals, Pipersville, PA). Titers were assessed by radioimmunoassay (RIA). One rabbit generated titers above 1:1,000; following a third injection of antigen, the rabbit yielded a high-affinity antiserum that was used at a 1:10,000 dilution.

Cell Culture, Isolation, and Purification of Mitochondria—Mouse Leydig (MA-10) cells were incubated in 15% horse serum, 5% fetal bovine serum, and 1 × gentamycin at 37 °C in a humidified incubator under 5% CO_2. Cells were removed from tissue culture plates by gentle scrapping using PBS. Cells were incubated in the hypotonic buffer 10 mM HEPES at pH 7.4 for 40 min prior to Dounce homogenization with 10 gentle up and down strokes. Cell debris was removed by spinning at 3,500 × *g* for 10 min. The supernatant containing the mitochondrial fraction was spun down at 10,000 × *g* for 10 min, and then the pellet was washed with the mitochondria isolation buffer. The washing step was repeated twice and the pellet was resuspended in energy regeneration buffer (125 mM sucrose, 80 mM KCl, 5 mM $MgCl_2$, 10 mM NaH_2PO_4, 10 mM sodium succinate, 1.0 mM ATP, 1.0 mM NADP, 0.1 mM ADP, 30 mM creatine phosphate, 1 mM creatine kinase and 25 mM HEPES, pH 7.4).

Biological Activity of Purified Proteins—Mitochondria were isolated from steroidogenic MA-10 cells following our established procedure as described (16, 17). For the metabolic conversion assays, mitochondria (300 mg) were incubated in potassium phosphate buffer along with 3 million cpm of [^{3}H]pregnenolone and then chased with 30 μg of cold progesterone. Metabolic activity was initiated by the addition of 0.01 M NAD and allowed to proceed for 4 h at 37 °C in a shaking water bath. To determine the effect of electrochemical gradient we incubated the mitochondria isolated from steroidogenic MA-10 cells with valinomycin (2 μg/ml), oligomycin (50 μg/ml), and carboxyatractyloside (50 μg/ml) for 3 h. To evaluate the effect of pH-mediated partial unfolding on metabolic

conversion, we incubated 3βHSD2 at a pH of 3.0, 3.5, 4.5, 5.5, and 7.4 for 1 h at room temperature prior to adding the mitochondrial incubation mixture. Similarly, we induced 3βHSD2 unfolding by incubating the protein for 30 min at room temperature with various concentrations of guanidinum hydrochloride (GdmHCl): 10 mM, 20 mM, 50 mM, 100 mM, 200 mM, 500 mM, 1 M, and 2 M. At 200 mM, GdmHCl induces partial unfolding, whereas at 1.75 M, unfolding reaches a plateau; thus, we assumed that 200 and 500 mM GdmHCl would induce an intermediate state of unfolding. After addition of all of the assay components, the reaction was incubated for 3 h at 37 °C in a shaking water bath. Steroids were then extracted in ether/acetone, 9:1. Signal intensity was determined by a phosphorimager. We characterized all the steroids by gas chromatography/mass spectrometry.

Gas Chromatography-Mass Spectrometry—The spots extracted from TLC plates were subjected to GC-MS analysis on an Agilent 7890 GC with 5975C mass spectrometer. The column used was an Agilent HP-5 with dimensions 30 m × 0.25-mm inner diameter with a 0.25-μm film thickness. Samples were dissolved in 50 μl of dichloromethane and 1 μl was injected onto the column using a pulsed splitless injection. Helium was used as the carrier gas at a flow rate 1 ml/min. The temperature program is as follows: ramp at 10 °C/min from 70 to 310 °C and hold for 6 min. Spectra were collected in full scan mode with 70 Ev ionization over the mass range *m*/*z* 50 to 500 to facilitate comparison of MS spectra with the NIST/EPA/NIH NIST08 mass spectral library.

Circular Dichroism (CD)—CD experiments in the far-UV region (195–250 nm) were carried out using a 1.0-mm pathlength quartz cuvette at 20 °C in a Jasco J-815 spectropolarimeter equipped with a Peltier temperature-controlled cell holder and a four-syringe stopped flow (New Biologic System). The instrument was purged with a continuous flow of nitrogen of 20 liter/min to reduce the maximum signal to noise ratio. The CD spectra obtained in the near-UV (250–375 nm) were recorded in a 1-cm path length cuvette with a protein concentration of 2.0 mg/ml. Spectra obtained in the far-UV are presented without mathematical smoothing. Purified wild-type 3βHSD2 was equilibrated in NaH_2PO_4 buffers ranging in pH from 2.5 to 7.4, and the CD spectra were recorded as a function of pH. The mean residue molar ellipticity [Θ] at 208 and 222 nm was plotted *versus* pH. Secondary structural analysis was carried out using the CD-Pro (18–21) to determine the relative proportions of α-helix and β-sheet as a function of pH. In a separate set of experiments, purified wild-type 3βHSD2 was equilibrated in 10 mM sodium phosphate at pH 3.0, 3.5, 4.0, 4.5, and 7.5, prior to any experiments, and aggregation was removed by centrifugation at 100,000 × *g* for 1 h and recording the optical density before and after centrifugation. Temperature-dependent unfolding was measured at 222 nm where the temperature was increased from 4 to 80 °C. For pH-mediated or GdmHCl-mediated unfolding, the appropriate buffer blank was subtracted from each spectrum, and Θ at 222 nm was plotted with respect to the pH of solution or GdmHCl concentration.

Measurement of ANS-3βHSD2 Binding—Steady state fluorescence experiments were performed using a Hitachi (Hitachi, Model F-7000) spectrofluorometer using a 10-mm path length quartz cuvette. Fluorescence spectra for 1-anilinonaphthalene-8-sulfonic acid (ANS) were recorded at an excitation of 357 nm with 5-nm band pass slits for both excitation and emission channels. All experimental values were corrected for those obtained for buffer 10 mM NaH_2PO_4 at pH values of 3.0, 4.5, 5.5, and 7.5, and free ANS run under identical conditions. The sample temperature was maintained at 22 °C for all experiments unless otherwise indicated. Stock solutions of 400 μM ANS in Me_2SO were diluted into water, and the concentration was determined using a molar absorption coefficient (ϵ) of 4990 M^{-1} cm^{-1} (22). Protein-ANS dissociation constants were determined by nonlinear curve fitting of the binding isotherm based on the following equilibrium: $L + P \times L - P$, where *L* and *P* are ANS and protein, respectively. ANS binding experiments were performed using 14 μg of protein, to which increasing amounts of ANS were added, and the emission intensity was measured at 470 nm to monitor protein-bound ANS in 15 different data points. The data points obtained from fluorometric titrations were analyzed by fitting to Equations 1 and 2. A total of 15 data points were recorded with a fixed increase in ANS concentration of 1 μM while the maintaining protein concentrations remained unchanged. The dissociation constants of ANS binding to 3β*HSD*2 (K_d) were determined by nonlinear curve fitting analysis using Equation 2 (22). All of the experimental points for the binding isotherm were fitted by least square analysis using a Microcal Origin software package (version 6.0, Microcal Software Inc., Northampton, MA). The binding stoichiometries of the ANS-protein complex were estimated from the intercept of two straight lines of the nonlinear fitted plot of $\Delta F/\Delta F_{max}$ against the mole fraction of ANS.

$$K_d = [C_0 - (\Delta F/\Delta F_{max})C_0][C_p - (\Delta F/\Delta F_{max})C_0]/(\Delta F/\Delta F_{max})C_0 \quad \text{(Eq. 1)}$$

$$C_0(\Delta F/\Delta F_{max})2 - (C_0 - C_p + K_d)(\Delta F/\Delta F_{max}) + C_p = 0 \quad \text{(Eq. 2)}$$

In both equations, ΔF is the change in fluorescence emission intensity at 470 nm (λ_{ex} = 360 nm) for each point on the titration curve, and ΔF_{max} change in fluorescence emission intensity when the protein is completely bound to ANS. C_p is the concentration of the ANS, and C_0 is the initial concentration of protein. The double reciprocal plot was used to determine ΔF_{max} following Equation 3, and determined the apparent binding constant (K_{app}) (23).

$$1/\Delta F = (1/\Delta F_{max}) + 1/[K_{app}\Delta F_{max}(C_0 - C_p) \quad \text{(Eq. 3)}$$

The linear double reciprocal plot of $1/\Delta F$ against $1/(C_p - C_0)$ is extrapolated to the ordinate to obtain the value of ΔF_{max} from the intercept. The apparent binding constant, K_{app}, is the inverse of the dissociation constant (K_d). The approach is based on the change in emission intensity of ANS is proportional to the concentration of the protein. C_p and C_0 represents protein (14 μg) and ANS concentrations. Thus, the apparent binding rates reflect the ANS effect at the molten globule core as described from the changes with the incremental addition of ANS.

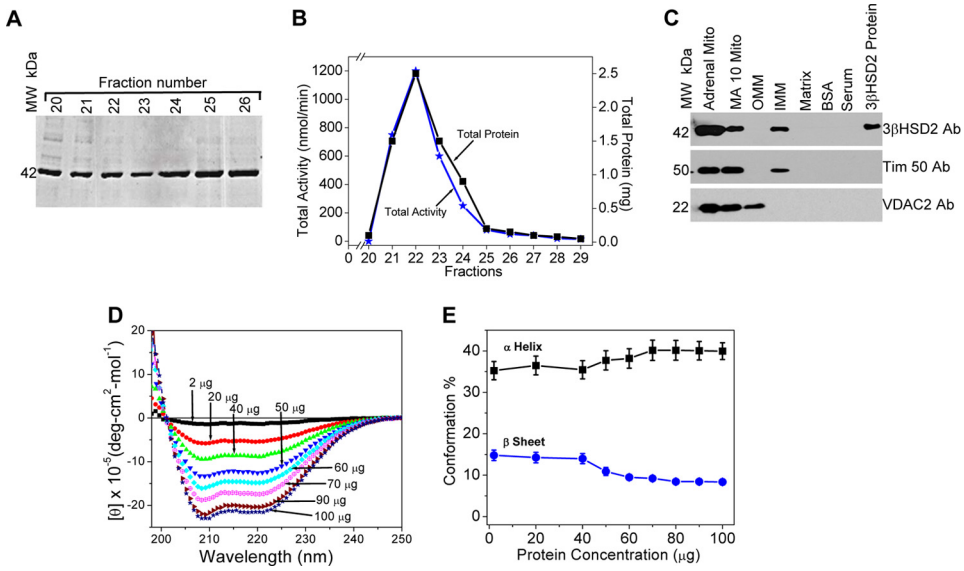

FIGURE 1. **Purification, biological activity, and characterization of recombinant 3βHSD2 protein.** *Panel A*, SDS-PAGE expression profile of baculovirus-expressed human 3βHSD2 purified from Sf9 cells by DEAE ion exchange followed by hydroxyapatite chromatography and stained with Coomassie Blue. The crude expression is designated as wild-type of molecular mass 42 kDa. The *lane numbers* show the fractions from the hydroxyapatite column. *Panel B*, activity of the different fractions of 3βHSD2 purified through the hydroxyapatite column used for detergent exchange. The activity was measured spectrophotometrically through the conversion of 5-androstene-3,17-dione to androstenedione, fractions 21–24 were pooled as the final preparations of pure 3βHSD2 in the UV-visible, high CMC detergent Cyamal-5. *Panel C*, Western blot of mitochondrial (*Mito*) fractions from steroidogenic MA-10 cells probed with human 3βHSD2 antibodies, where 3βHSD2 remains associated with the IMM. The *middle* and *lower panels* show the accuracy of the identification of 3βHSD2, when the same membrane was probed with IMS resident Tim50 and OMM resident VDAC2 antibodies. *Panel D*, an equilibrium CD of fraction 22 was recorded with a 50-fold difference in concentration, from 2 to 100 μg, at 20 °C. *Panel E*, analysis of the change in α-helix and β-sheet conformation with an increase in protein concentration. The helical content remained nearly unchanged at all the concentrations. Data presented in *panel E* are the mean ± S.E. of three independent experiments.

Stabilization of 3βHSD2 with Specific Detergent—Igepal CO 720, a polyoxyethylene phenyl ether nonionic detergent that has phenyl groups, eluted the enzyme from a DEAE ion exchange column with a very sharp peak during purification. To determine whether the Igepal CO 720 detergent can promote stabilization, we added different concentrations of this detergent to a fixed concentration of 3βHSD2 and then determined the stoichiometry of binding by recording the equilibrium CD at 190–250 nm. The detergent itself has strong absorption at 205 nm, and thus the signal to noise ratio is higher in this region. To circumvent this problem, we determined binding at 208 and 222 nm.

Stopped-flow Kinetics—The kinetics of protein unfolding were measured in a JASCO-815 spectropolarimeter interfaced with an SF4 stopped-flow module (Biologic, France). A stock concentration of 3βHSD2 (2.0 mg/ml) in the syringe was changed to 0.1 mg/ml in the cell. For acid-mediated unfolding, 3βHSD2 (25 μl) and varying amounts of buffer at different pH values were mixed with a "Delta" mixer so that the protein concentration remained unchanged, but the pH decreased to 3.0, 3.5, 4.0, 5.5, and 7.4. For acid gradient unfolding, varying amounts of 10.0 mM NaH_2PO_4, pH 3.0, in a second syringe and water in the third syringe were mixed in such a fashion that the pH of the solution changed without significant interruption of the ionic concentration of the protein. The syringes were operated 10.0 ml/s with a 6.8-ms dead time. Fluorescence was measured by excitation at 280 nm with emission intensity using a 320-nm cutoff filter. Data were collected in four segments. First, 5 data points were collected to monitor the basal signal of the solution. Second, the solution was mixed for 60 ms. Third, 100 data points were collected over 100 ms to monitor initial rapid kinetics, then 200 data points were acquired over a 2-s time period to monitor slow kinetics (24).

RESULTS

3βHSD2 Protein Does Not Aggregate at Higher Concentrations—To characterize 3βHSD2, we expressed the protein in the baculovirus system and then purified it from Sf9 cells in the presence of the low-CMC detergent, Igepal CO 720, using a DEAE ion exchange column. Coomassie Blue staining of fractions separated by SDS-PAGE (12%) revealed a single band (42.0 kDa) that co-migrated with the crude 3βHSD2 extract (Fig. 1*A*). To facilitate analysis of protein folding, the Igepal detergent was replaced with the high-CMC detergent Cymal-5 using hydroxyapatite column chromatography. Based on enzymatic assay, we determined that the peak binding capacity occurred in fractions 20–26, indicating active 3βHSD2 (Fig. 1*B*). To confirm the mitochondrial localization, we stained fractionated mitochondria from steroidogenic MA-10 cells with our human 3βHSD2 antibody. 3βHSD2 was present only in the IMM fraction and was resistant to proteolysis. Probing the same membrane with antibodies directed against OMM-associated voltage-dependent anion channel 2 (VDAC2) and IMM-associated Tim50 confirmed the association of 3βHSD2 with the IMM (Fig. 1*C*).

Many proteins change their conformation and/or form aggregates at high concentrations. The signal intensities of CD spectra obtained in far-UV for this preparation of 3βHSD2 at pH 7.5 depended solely on concentrations over a 50-fold range, from 2 to 100 μg (Fig. 1*D*). The CD data gave a linear correlation between concentration and Θ at both the π-π^* transition at 208 nm and the n-π^* transition at 222 nm (Fig. 1*D*). Thus, the bio-

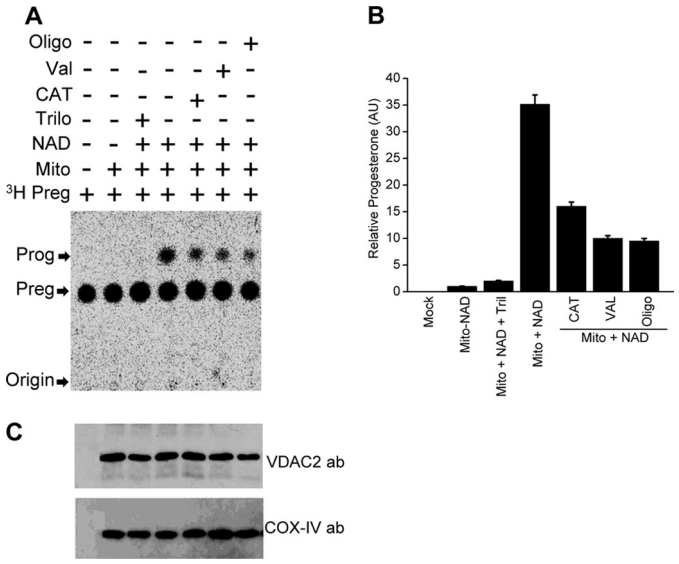

FIGURE 2. **Effect of electrochemical gradient on 3βHSD2 activity.** *Panel A*, metabolic conversion of pregnenolone to progesterone from the isolated mitochondria (*Mito*) of MA-10 cells in the absence and presence of carboxyatractyloside (*CAT*), oligomycin (*OLIGO*), and valinomycin (*VAL*). *Panel B*, quantitative estimation of the metabolic conversion as identified in *panel A*. *Panel C*, Western blot of the cells with the indicated antibodies after incubation with valinomycin, oligomycin, and carboxyatractyloside.

logically active 3βHSD2 protein employed in this study did not aggregate or change its conformation at this pH. Computational analysis with increasing 3βHSD2 concentrations showed (Fig. 1*E*) a minor increase in α-helical content at or above 40 μg. At the same time, β-sheet content decreased from 15 to 10% when the protein concentration increased from 40 to 60 μg, and then remained unchanged with further increases in concentration. The observation that the protein did not aggregate at 100 μg supports the notion that, due to the intramolecular interaction, the change in β-sheet content occurs at the expense of maintaining the entropy of the protein.

Effect of Electrochemical Gradient on 3βHSD2 Activity—To investigate the role of electrochemical gradient at the IMS, we have determined activity with the mitochondria isolated from the MA-10 cells incubated with various electrochemical gradient inhibitors: oligomycin inhibits the H^+-translocating ATP; valinomycin collapses electrochemical potential across the inner membrane; and carboxyatractyloside inhibits access of ATP to the matrix (25–27). Oligomycin and valinomycin, but not carboxyatractyloside, inhibited conversion from pregnenolone to progesterone (Fig. 2*A*). Because of the inhibition of proton pump at the IMS no metabolic conversion is possible. A quantitative estimation of the intensity of bands (Fig. 2*B*), as measured by the PhosphorImager, shows that incubation with carboxyatractyloside retained 45% activity, whereas incubation with valinomycin and oligomycin retained ~22%. As a control we also performed Western blot analysis with different antibodies on the mitochondria after incubation with the different inhibitors. For OMM-associated expression, we probed with the VDAC2 antibody and matrix proteins with the COX IV antibody. The Western blot shows (Fig. 2*C*) that the expression of VDAC2 and COX IV is unchanged suggesting that the addition of these inhibitors did not reduce mitochondrial architecture.

Effect of pH on 3βHSD2 Conformation—CD spectroscopy can distinguish secondary structural components by the presence of minima near 198 nm for random coil, at 208 and 222 nm for the α-helices, and 218 nm for β-sheets (28, 29) and so changes in the CD spectra were used to monitor pH-induced unfolding of 3βHSD2 (Fig. 3*A*). We found that the CD spectrum generally remained unchanged from pH 7.4 down to pH 4.5, indicating that the protein retained its predominately α-helical character. However, at pH 4.5, there was a minor reduction in ellipticity at the 208 nm π-π^* position. With a further decreases in pH, the ellipticity remained almost unchanged at the 222 nm n-p^* position, but changed significantly at the 208 nm π-π^* position. At pH 3.0 or 2.5, the protein conformation changed to a random coil. Secondary structural analysis (18–21) clearly shows the effect of pH on 3βHSD2 conformation (Fig. 3*B*): decreasing the pH to 3.25 resulted in a decrease in the α-helical conformation without a significant change in the β-sheet conformation. When the pH was titrated back from pH 3.25 to 7.4, the conformation was restored (Fig. 3*C*), suggesting that conformational changes were reversible. However, titrating back the pH from 3.0 to 7.4 did not restore the initial conformation, and thus the complete denaturation to random coil may have destroyed protein flexibility. Based on these observations, pH 3.25 appears to represent the threshold for 3βHSD2 to maintain a reversible, flexible conformation (Fig. 3*D*). This range in pH resembles the mitochondrial proton gradient, which supports the possibility that mitochondrial resident 3βHSD2 undergoes conformational changes associated with the proton gradient.

Effect of pH on Progesterone Synthesis—To evaluate if the change in pH alters 3βHSD2 activity, we measured the conversion of pregnenolone to progesterone. 3βHSD2 protein (20 μg) was equilibrated with the appropriate pH buffer and then incubated with isolated mitochondria from steroidogenic MA-10 cells. We normalized progesterone levels to the amount produced in the absence of the cofactor, NAD (0.01 M). At pH 4.5, 3βHSD2 synthesized 25% progesterone, the highest level, whereas at pH 7.4 3βHSD2 only synthesized 11%, similar to the amount at pH 3.5 (Fig. 4*A*). This experiment clearly indicates that pH 4.5 supports the maximum level of 3βHSD2 activity.

We next addressed whether the 3βHSD2 protein concentration affected the level of metabolic activity seen at the different pH values. Fig. 4*B* demonstrates that 3βHSD2 at pH 7.4 increased progesterone synthesis with an increase in protein concentration. However, 3βHSD2 activity at other pH values exhibited varying degrees of sensitivity to protein concentration. We observed that 3βHSD2 (40 μg) produced 35% relative progesterone at pH 4.5, 28% at pH 5.5, and 10% at pH 3.5. At a concentration of 100 μg of 3βHSD2, the relative amount of progesterone produced decreased slightly at pH 5.5, remained similar at pH 7.4, and substantially increased at pH 4.5. These observations corroborate our previous finding that pH 4.5 supported the most active state of the protein. At the other pH values, more than 40 μg of 3βHSD2 had no significant effect on the catalytic conversion, suggesting that the large amount of protein may have blocked the mitochondrial metabolic transport by partially blocking the import channel and thus become ineffective (Fig. 4, *B* and *C*). This did not appear to be the case for

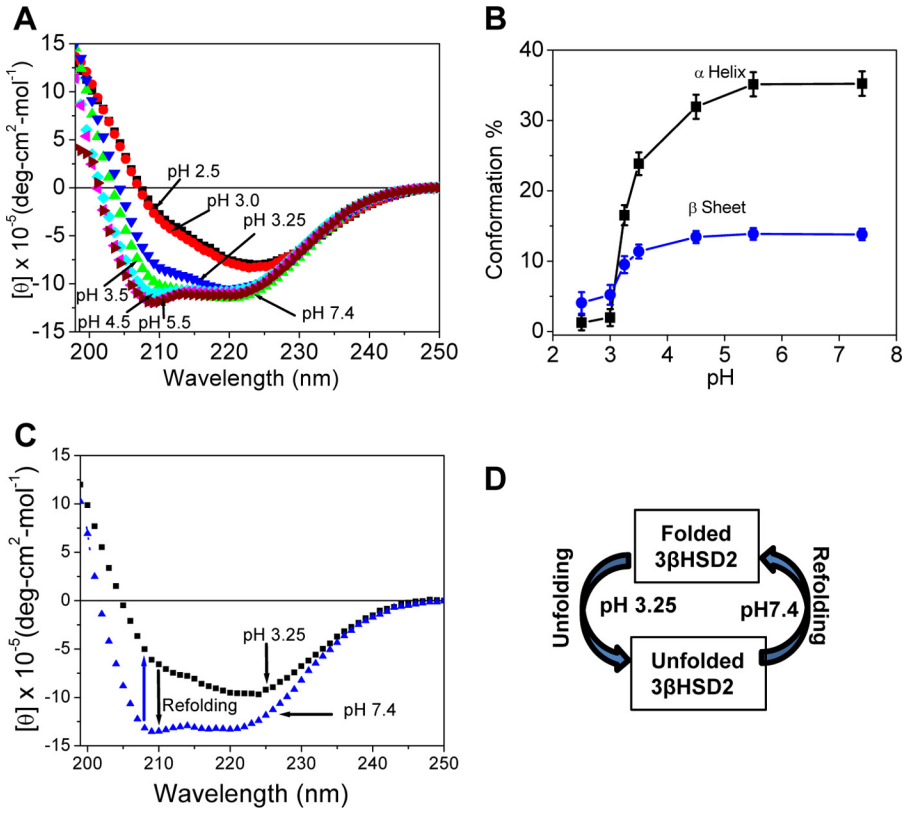

FIGURE 3. **Effect of pH on protein conformation.** *Panel A*, far-UV CD of 3βHSD2 protein recorded between 195 and 250 nm and equilibrated at the pH indicated in the spectrum. *Panel B*, analysis of the change in α-helix and β-sheet conformation with change in pH, indicating that α-helical composition changed at or below pH 4.0, whereas the β-sheet changed at or below pH 3.5. *Panel C*, the spectrum after titrating back the pH from 3.25 to 7.4 shows that the conformation between pH 3.25 to 7.4 was reversible. *Panel D*, schematic depicting the reversible conformation attained in *panels A* and *C*.

pH 4.5 as the mitochondria did not show signs of saturation. Rather, at this pH, the limiting factor appeared to be the catalyst.

We next measured the kinetics of progesterone synthesis at either pH 7.4 or 4.5 using a fixed amount of 3βHSD2 (40 μg). Synthesis at either pH started at about 30 min, but the amount of progesterone produced at pH 4.5 was 2-fold more than that at pH 7.4 (Fig. 4, *D* and *E*). Within 2 h, synthesis reached its saturation point at pH 7.4. At pH 4.5, synthesis at 1 h yielded 3-fold more progesterone than at pH 7.4. The synthesis at pH 4.5 did not reach saturation until 4 h, and the amount produced was more than 6-fold its initial synthesis (Fig. 4, *D* and *E*). The radioactive pregnenolone and its metabolite(s) (Fig. 4, *B* and *D*) were characterized by GC-MS. The samples scraped from the TLC plate were dissolved in dichloromethane and analyzed on the GC-MS instrument (supplemental Fig. S1, *A–D*). Supplemental Fig. S1*A* shows the extracted ion chromatogram for the molecular ion of pregnenolone at *m*/*z* 316.2. Supplemental Fig. S1*B* shows the full scan mass spectrum at a retention time (RT) of 21.02 min. This matched the NIST08 library and identified pregnenolone with a quality factor of 99/100. Supplemental Fig. S1*C* shows the extracted ion chromatogram for the molecular ion of progesterone at *m*/*z* 314.2 and supplemental Fig. S1*D* shows the full scan mass spectrum at a RT of 21.90 min. This spectrum matched the NIST08 library with a match for progesterone with a quality factor of 96/100. The spectral match to the NIST08 library confirms that spots from the TLC plate contained the expected steroid. In all, these observations provide further support that the unfolded state of 3βHSD2 has higher activity. To further confirm this, we performed a metabolic conversion assay at pH 7.4 in the presence of different concentrations of the chaotropic agent, GdmHCl (Fig. 5*A*) in the presence of mitochondria isolated from MA-10 cells. Concentrated GdmHCl disrupts the higher structure of water, decreasing hydrophobic effects and promoting protein unfolding and dissociation. Addition of 10 mM GdmHCl increased progesterone synthesis, and at 200 mM GdmHCl, relative progesterone levels were 4-fold greater than levels measured in the absence of GdmHCl (Fig. 5*A*). Peak synthesis of 7-fold occurred with 200 mM GdmHCl and then subsequently declined until there was a complete loss of activity at 2 M GdmHCl (Fig. 5*B*), likely due to the denaturation of 3βHSD2. These results confirm that 3βHSD2 exhibits peak activity when in a partially open conformation (Fig. 5*C*).

Cooperative Denaturation—To better understand why partial unfolding of 3βHSD2 led to increased activity, we evaluated the effects of acidic and GdnHCl cooperative denaturation on the protein. Fig. 6*A* shows GdnHCl denaturation curves obtained at pH 3.5, 4.0, 4.5, 5.5, and 7.4. As compared with the melting curve from proteins at pH 7.4, all the curves exhibited a decrease in ellipiticity. This decrease may represent the protein transitioning from the native folded state to the intermediate ion core state due to the presence of long hydrophobic amino acids at the N terminus. In addition, pH 3.5 may represent the threshold pH before complete denaturation (Fig. 6*A*). The melting curves at pH 7.4, 5.5, and 4.5 show that the protein at those pH values underwent a three-step transition, suggesting that a small decrease in pH could not open the hydrophobic

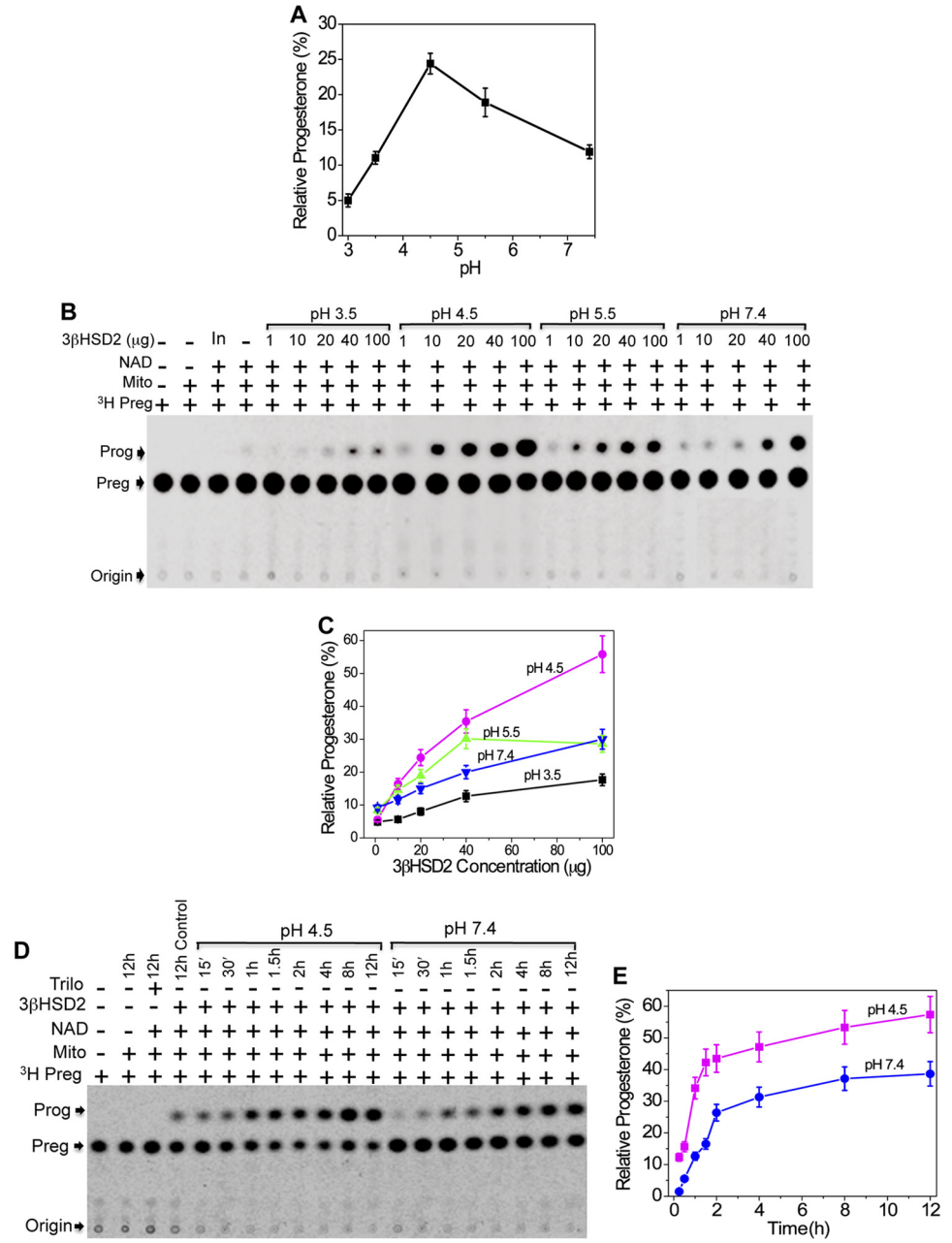

FIGURE 4. **Metabolic conversion of [^{3}H]pregnenolone to [^{3}H]progesterone after incubation of 3βHSD2 pre-equilibrated at different pH values.** After pre-equilibration, 3βHSD2 was further incubated with the isolated mitochondria (*Mito*) from MA-10 cells, [^{3}H]pregnenolone and NAD for an additional 3 h (unless otherwise indicated) and then metabolites were separated by thin-layer chromatography. *Panel A*, pregnenolone to progesterone conversion where 3βHSD2 was previously equilibrated at the indicated pH values. The amount of conversion was measured by PhosphorImager, normalized to levels synthesized in the absence of NAD, and plotted against pH. The activity was maximum at pH 4.5. *Panel B*, thin layer chromatogram showing the measurement of progesterone conversion with different concentrations of 3βHSD2 pre-equilibrated at the indicated pH. The activity was maximum at pH 4.5 and saturation was not evident at that pH. *Panel C*, quantitation of radioactive conversion observed in *panel B*. *Panel D*, thin layer chromatogram showing the conversion of (pregnenolone to progesterone) kinetics at pH 7.4 and 4.5. The result shows that synthesis began at 30 min for proteins equilibrated to either pH. Over time, 3βHSD2 pre-equilibrated to pH 4.5 synthesized more progesterone than protein at pH 7.4: at 1 h 3βHSD2 at pH 4.5 synthesized 2-fold more and at 3 h the amount increased to 7-fold more. Saturation was reached at 8 h for the 3βHSD2 at pH 4.5. *Panel E*, quantitative analysis of the progesterone conversion from *panel D*. Data presented in *panels A*, *C*, and *E* is the mean ± S.E. of three independent experiments.

core of 3βHSD2. Based on the melting curves, we calculated ΔG and plotted it as a function of GdmHCl concentration (Fig. 6*B*). For 3βHSD2 equilibrated to pH 7.4, addition of GdmHCl at concentrations greater than 0.2 M resulted in ΔG decreasing from 1.5 to −5.4 kcal/mol. After the initial opening, the decrease in ΔG −5.4 kcal/mol may be the result of the participation of very loose amino acids from the peripheral side of the domains involved in relatively tighter folding. Increasing concentrations of GdmHCl, from 0.2 to 1.75 M, caused the protein to undergo a very slow, cooperative transition. The second cooperative change, beginning at 1.75 M GdmHCl, was faster than the first change. At pH 7.4, the unfolding was completed at 3.5 M GdmHCl. Thus, the protein needs to undergo a very slow, smooth cooperative unfolding for pH 7.4 and 5.5 prior to its complete denaturation. The three-step transition also exists for pH 4.5, but it is subtle because of the already attained partially

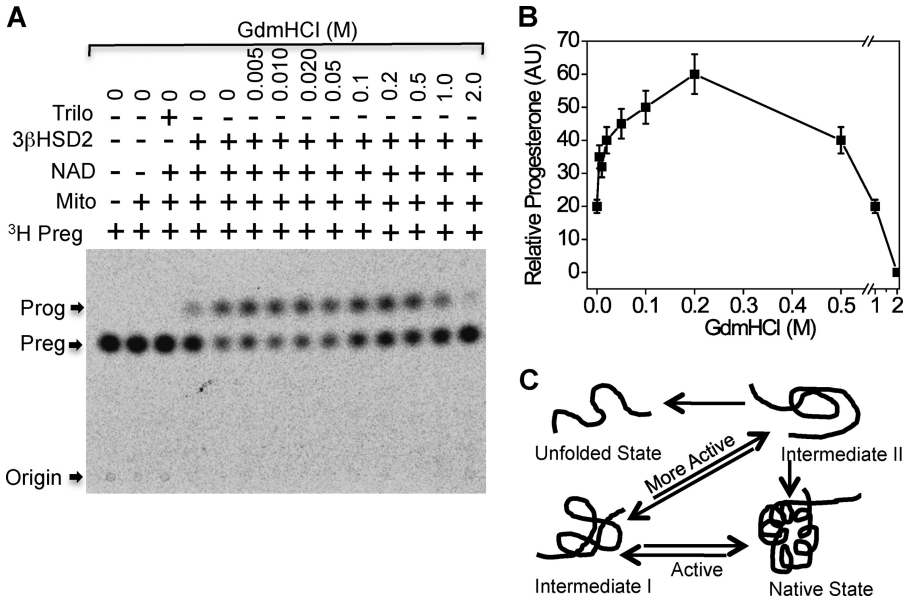

FIGURE 5. **Metabolic conversion of [^{3}H]pregnenolone to [^{3}H]progesterone after incubation of 3βHSD2 pre-equilibrated at different concentrations of GdmHCl.** *Panel A*, pregnenolone conversion using 3βHSD2, pH 7.4, that had been incubated overnight with various concentrations of GdmHCl. Enzyme activity reached its peak with 200 mM GdmHCl. *Panel B*, summary of the results showing that the most active intermediate form of enzyme was achieved with pH 4.5 or with 200 mM GdmHCl at pH 7.4 from *panel A*. Data presented in *panel B* are the mean ± S.E. of three independent experiments. *Panel C*, summary of the results from *panel B*. Addition of GdmHCl partially unfolded the protein, which was more active than the native state. The initial unfolded intermediate state (*intermediate state I*) may be unfolded further (*intermediate state II*) and these states were reversible. Further unfolding with an increase in GdmHCl concentration brought 3βHSD2 to the completely unfolded and inactive form.

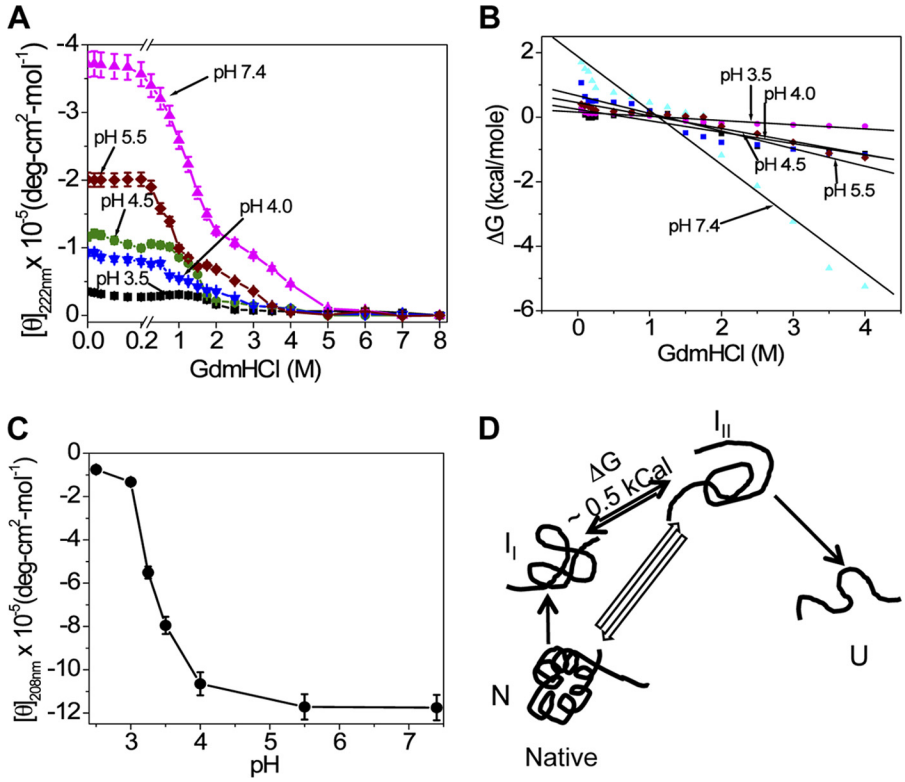

FIGURE 6. **Denaturation of 3βHSD2 by GdmHCl.** *Panel A*, equivalent amounts of 3βHSD2 were equilibrated overnight with varying concentrations of GdmHCl buffered with 50 mM NaH_2PO_4 at pH values from 3.0 to 7.4. The ellipticity at 222 nm was recorded in a 1.0-mm path length cuvette at 20 °C and plotted against the GdmHCl concentration, as determined by the refractometer. The *curves* show three-step unfolding at pH 7.4 (▲, *pink*), 5.5 (◆, *red*), and 4.5 (■, *green*) and others at pH 4.0 (▼, *blue*) and 3.5 (■, *black*). *Panel B*, free energy change (Δ*G*) as a function of GdmHCl concentration. The Δ*G* was calculated from the *panel A*. Δ*G* values for pH 7.4 (▲, *pink*) are 0.72 and −2.1, for pH 5.5 (◆, *red*) are 0.15 and −0.5, for pH 4.5 (■, *green*) is 0.08, for pH 4.0 (▼, *blue*) is 0.07 and for pH 3.0 (■, *black*) is 0.3. *Panel C*, change in ellipticity (*y* axis) was plotted with pH (*x* axis). *Panel D*, the schematic presentation shows that the native 3βHSD2 protein (*N*) undergoes conformational changes to two intermediate states that are in equilibrium, I_I and I_{II}, prior to complete unfolding (*U*).

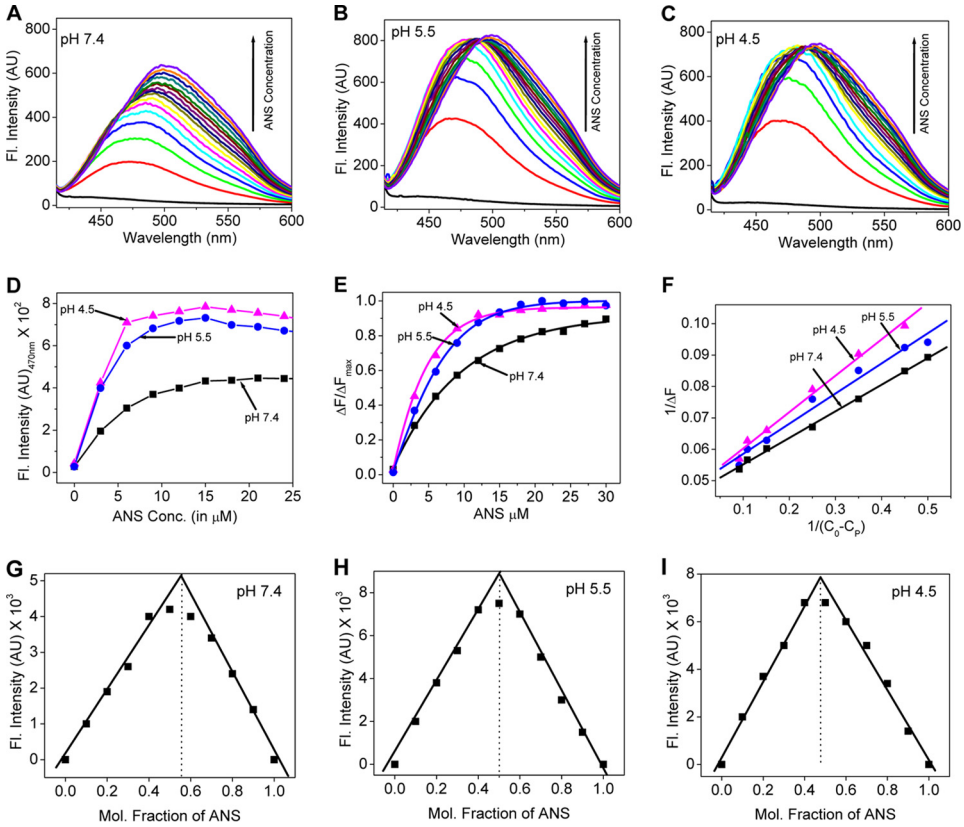

FIGURE 7. **Measurement of molten globule state by ANS.** Fluorescence emission spectra of ANS binding to 3βHSD2 as a function of pH. *Panel A*, fluorescence spectra of ANS binding to 3βHSD2 at pH 7.4; *panel B* at pH 5.5; and *panel C* at pH 4.5. *Panel D*, fluorescence intensity at 470 nm plotted against the ANS concentration. *Panel E*, the relative ratio of ANS binding ($\Delta F/\Delta F_{max}$) at pH 7.4, 5.5, and 4.5. *Panel F*, plot of the reciprocal of the difference in intensity (ΔF) against the reciprocal of the difference in the initial (C_0) and final concentration (C_p) of ANS to determine the apparent binding constant. *Panels G–I*, determination of the binding stoichiometry between ANS and 3βHSD2 by Job's plot at pH 7.4 (*panel G*), 5.5 (*panel H*), and 4.5 (*panel I*).

open conformation at the lower pH. The change in ΔG from 1.5 to −5.4 kcal suggests that the protein did not have tight shielding, from pH 7.4 to 4.5, prior to the start of the cooperative unfolding. At lower pH values, increasing GdmHCl concentrations resulted in a two-step, rapid unfolding, possibly due to the complete loss of structure.

These curves fit a multiple state model (Fig. 6*D*) in which the free energy differences between the native (N) and unfolded (U) conformations depend linearly on the concentration of the denaturant; thus $\Delta G = \Delta G_{H2O} - m$(GdmHCl), where ΔG is the apparent free energy difference at any GdmHCl concentration, ΔG_{H2O} is the free energy difference in the absence of denaturant, and m is a parameter describing the cooperativity of the transition. Hence, at pH values between 3.25 and 4.5, ΔG_{H2O} = 1.95 kcal/mol and m = 0.9 kcal and higher values from pH 4.5 to 7.4. ΔG changed from 1.67 to −5.4 kcal/mol, but the nature of the two-step cooperative denaturation remained unchanged (Fig. 6*B*). A plot of ellipticity with pH shows retention of increased structures with an increase in pH (Fig. 6*C*). The loss of the ellipticity may be due to the putative loosely folded conformation of the outer core of the protein. The conclusion that the inner core remained intact indicates that the tightly folded inner core is shielded by loosely folded domains of the inner core. Thus, loss of the outer sphere of the protein at pH 4.5 may allow interactions between the unfolded inner core and mitochondrial membrane to occur, promoting activity.

Unfolding States Analysis by ANS—To further confirm the notion that 3βHSD2 at a lower pH (pH 4.5) is partially unfolded and thus exhibits higher activity than when at its native conformation, we performed ANS binding with 3βHSD2 at different pH values (Fig. 7, *A–I*). ANS binds to hydrophobic regions of partially unfolded proteins exposed to solvents that induce a conformational change in the protein structure (30). In particular, ANS binds strongly to proteins in a molten globule structure (31). Binding of ANS to 3βHSD2 at pH values ranging from 4.5 to 7.4 (Fig. 7, *A–C*) suggests more binding at pH 4.5 and 5.5. Upon excitation at 357 nm and in the absence of protein, ANS shows a very low quantum yield emission intensity maxima at ~525. However, binding of ANS in the acidic region led to an increase in the emission intensity as well as a concomitant shift in the emission maximum (Fig. 7, *B* and *C*), indicating the presence of exposed hydrophobic groups. The increasing concentration of ANS to a fixed concentration of 3βHSD2 (14 μg) increased fluorescence intensity. The difference between Fig. 7, *A* and *B*, shows the complete shift of the equilibrium as the isosbestic point for pH 7.4 (Fig. 7*A*) to 5.5 (Fig. 7*B*) or 4.5 (Fig. 7*C*) is changed from 460 to 490 nm because of the stronger binding of ANS. The binding efficiency of ANS at pH 4.5 was at least 2-fold more than at pH 7.4 (Fig. 7*D*), suggesting that protein at an acidic pH has a more open or more unfolded conformation, resulting in greater binding. This greater binding was possibly due to the loosening of the tertiary interactions that

helps in exposing the hydrophobic groups. To further confirm the flexible conformation, we titrated ANS with 3βHSD2 and estimated binding by determining the difference in fluorescence at each concentration of ANS with respect to the fluorescence maxima ($\Delta F/\Delta F_{max}$). Fig. 7*E* shows that the ANS binding to 3βHSD2 was greater at pH 4.5 and 5.5 than at pH 7.4. Next, we determined the apparent binding constant for ANS binding to 3βHSD2 at different pH values (Fig. 7*F*). The apparent binding constant (K_{app}) at pH 4.5 and 5.5 was 4.4 and 4.1 × 10^5 M^{-1}, respectively. However, at pH 7.4 and 3.0, K_{app} was 2.9 and 1.8 × 10^5 M^{-1}, respectively. The higher apparent binding constant at acidic pH indicates a stronger interaction than what was seen at pH 7.4. Further analysis of the stoichiometry of 3βHSD2 binding to ANS is shown by a Job's plot (Fig. 7, *G–I*). Fig. 7, *G–I*, shows that the protein to ANS binding ratio at pH 4.5 was 1:1.3, (Fig. 7*I*), and at pH 5.5 this ratio was 1:1.1 (Fig. 7*H*). The intersection point of the two limiting lines of a Job's plot will yield the binding stoichiometry of a ligand (32). For example, if the intersection point occurs at a mole fraction of 0.5, this would indicate 1:1 binding stoichiometry. However, at pH 7.4, this ratio was 1:0.7 (Fig. 7*G*), indicating greater binding of ANS at an acidic pH and supporting our notion that 3βHSD2 at pH 4.5 is in a partially unfolded conformation.

Stability by Thermal Denaturation—To better understand the process of 3βHSD2 unfolding, we calculated the melting temperature (T_m) as a function of pH (Fig. 8). The protein at pH 7.4 started to unfold at 30 °C and was completely unfolded at 70 °C. For this pH, we calculated the T_m as 42 °C (Fig. 8*B*). Not surprisingly, reducing the pH to 5.5, which would contribute to unfolding, resulted in a T_m of 37 °C. A plot of T_m values *versus* pH shows that proteins at pH 5.0 to 4.0 had T_m values in close range, but with a steady decrease, indicating continuous unfolding (Fig. 8*C*). However, proteins in the pH range of 4.25 to 3.25 had almost identical T_m values; this plateau may indicate a pseudo stable conformation in which most of the secondary structure is preserved due to slower unfolding. Slower unfolding may serve as a way for the protein to maintain equilibrium with the native state. We have summarized the results in the form of a schematic (Fig. 8*D*). The protein is in an unfolded (U) state at pH 3.0 and remains in a pseudo stable (I_{1I}) conformation from pH 3.5 to 4.0. From pH 4.0 to 5.0, the protein arranges itself to the most open state conformation (I_1), prior to reaching its most stable native (N) state. Thus, $N \rightarrow I_1 \Leftrightarrow I_{II} \rightarrow U$ represents the change in 3βHSD2 conformation from the native state to the completely unfolded state, where the interchange between the I_1 and I_{II} states remain reversible.

At pH 7.4 to 6, 3βHSD2 was at its most stable, native (N) state. Decreasing the pH induced a slow unfolding and between pH 5.0 and pH 4.0, the protein adapts an open conformation (I_1) that has the highest enzymatic activity. A further decease in pH, from 4.0 to 3.5, results in a pseudo stable conformation (I_{II}). These intermediate I_1 and I_{II} states appear reversible. Below pH 3.5, the protein becomes irreversibly unfolded (U).

Stopped-flow Kinetics and Real Time Unfolding of 3βHSD2 Domains—To illuminate the mechanism of 3βHSD2 activity, we measured protein unfolding using stopped-flow spectrophotometry (Fig. 9, *A–C*). Stopped-flow devices can monitor the unfolding and refolding of a protein in real time, thus

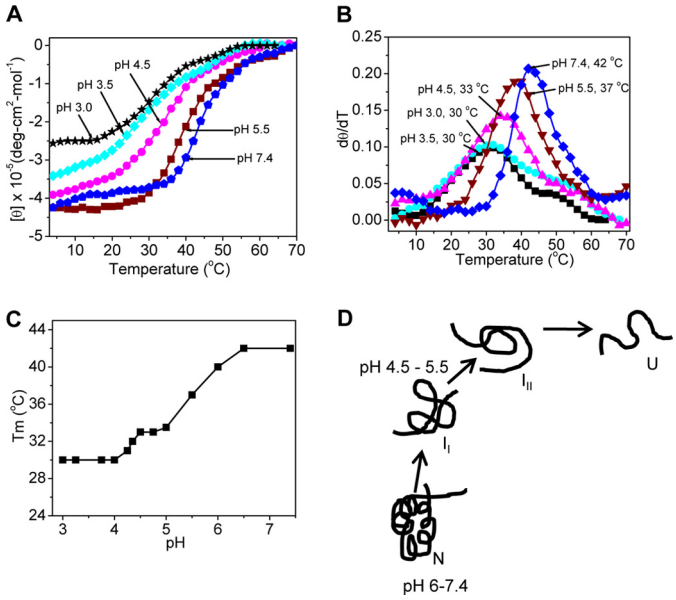

FIGURE 8. **Thermal unfolding of 3βHSD2 as a function of pH.** *Panel A*, thermal denaturation experiments were done by heating 3βHSD2 at the rate of 0.5 °C per min from 4 to 90 °C produced thermal transition curves when measured in a CD spectropolarimeter at 222 nm. For a simpler presentation, we have shown the data from 4 to 70 °C. 3βHSD2 was most stable at pH 7.4 with a T_m of 42 °C and least stable at or below pH 4.0. *Panel B*, the derivative of original thermal unfolding (T_m) indicates that the protein was most stable at pH 7.4 with a T_m of 42 °C and least stable at pH 3.0 with a T_m of 27 °C. *Panel C*, plot of the T_m observed with the change in pH. The *curve* shows that at pH 6 and above, the 3βHSD2 conformation is stable. Decreasing the pH caused a steady decrease in T_m, until T_m plateaus between pH 5 and 4.35. By pH 3, there is complete unfolding. *Panel D*, a schematic diagram illustrating the different states of 3βHSD2 as a function of pH. At pH 7.4 to 6, the protein is in its native state (*N*), which is most stable. The two intermediate states, I_I to I_{1I}, are at equilibrium between pH 5.5 and 4.5 and then the protein unfolds (U) at lower pH values.

revealing the different kinetic steps involved. The dead time or the mixing time of this instrument was set to 6.8 ms. The experiment requires rapid mixing of a protein in buffer with a high concentration of a denaturing agent such as urea or GdmHCl. Conformational changes in the protein are measured in milliseconds by fluorescence emission following excitation at 295 nm for Trp or at 280 nm for Trp and Tyr.

The unfolding kinetics appeared to be a single exponential process, and the values found by extrapolating back to time 0 agreed with those for the native state of the protein. When the buffers at different pH values are suddenly mixed, the protein starts to unfold, depending on the degree of denaturation. The rapid unfolding phase is defined as the "burst phase," which may or may not entail complete unfolding. The unfolding is completed when there is no change in fluorescence emission. The unfolding of 3βHSD2 occurred after the burst phase, not within the dead time for all pH values, except pH 7.4, which shows only diffusion. As measured by fluorescence emission, the time of unfolding ($t_{½}$) at pH 3.0 was 13 s with a relaxation time of 50 s (Fig. 9*A*), demonstrating that 3βHSD2 unfolds by a two-step process. Under similar conditions, the unfolding at pH 3.5 was slower, with an initial relaxation of 20 s (Fig. 9*B*). At higher pH values, 3βHSD2 might have been shielded by the flexible domains outside the core. Indeed, at pH 5.5 the protein gradually opened as shown by the $t_{½}$ of 45 s, and then underwent diffusion (Fig. 9*C*). Thus, the burst phase is buried within the relaxation phase. As expected, faster

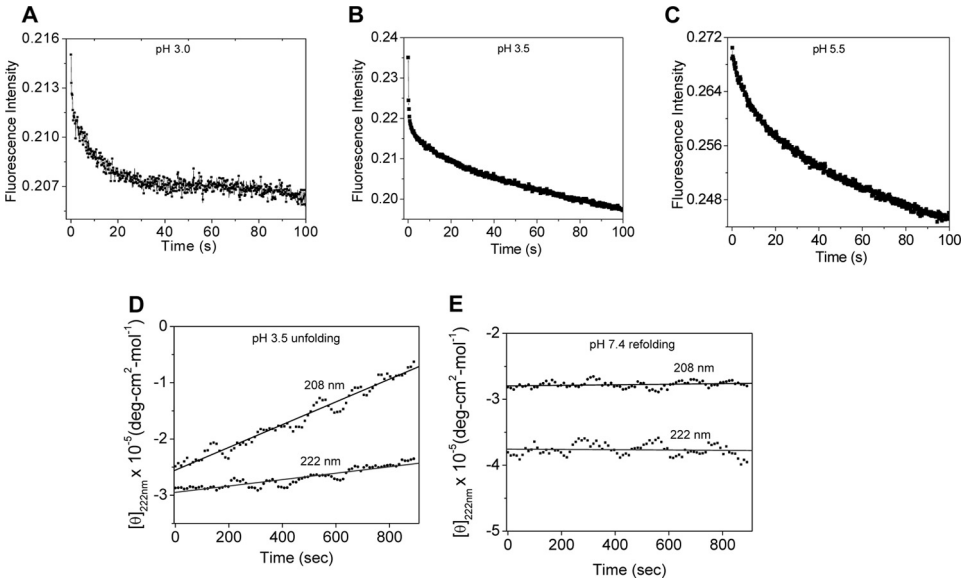

FIGURE 9. **Rate of unfolding by stopped-flow kinetics.** *Panels A–C*, the unfolding kinetics of 3βHSD2 were measured at different pH values, but for clarity only unfolding at pH 3.0, 3.5, and 5.5 are presented. *Panels D* and *E*, titrating the pH back from 3.5 (*D*) to 7.4 (*E*) resulted in the refolding of the protein within 25 min.

unfolding was observed at pH 3.25 and 4.0 (supplemental Fig. S2, *A* and *B*). However, at a further increase in pH to 7.4, no unfolding was observed, but only a slow diffusion (supplemental Fig. S2*C*). Thus, the slow unfolding at pH 5.5 suggests that there are no rearrangements during unfolding (33). The burst phase of unfolding shows no energy jump, confirming the rearrangement must have to open between pH 3.25 and 4.5, which remained in the molten globule state as indicated by the thermal denaturation (Fig. 8, *C* and *D*).

We also examined the reversibility of the unfolding. CD kinetic measurements at both 208 and 222 nm indicate that 3βHSD2 unfolds at pH 3.5 with increasing time (Fig. 9*D*). Also, a gradual decrease in negative ellipticity at 208 nm with increasing time shows the significant loss of α-helices at pH 3.5. However, the immediate development of negative and positive ellipticities around 208 and 222 nm, respectively, shows that the helical conformation was restored back after a pH jump from 3.5 to 7.4 (Fig. 9*E*) and the threshold limit for returning back to its original conformation was 25 min.

DISCUSSION

We had previously found that the steroidogenic enzyme, 3βHSD2, does not get cleaved upon import into the mitochondria. Rather, the N-terminal mitochondrial leader sequence directs the N terminus to enter the mitochondrial membrane. 3βHSD2 does so in an unfolded state. It then translocates to the IMM, where it associates with IMS proteins, but does not integrate into the membrane (3). This suggests that 3βHSD2 may lack a receptor, which would allow greater flexibility of the protein. The proton pump can also be found at the IMM. The electrochemical gradient produced by the proton pump results in localized change in pH. Because 3βHSD2 associates with the IMM, we posit that the protein faces the proton gradient and likely remains partially unfolded.

To test whether pH modulates the 3βHSD2 conformation, we equilibrated purified protein at different pH values and evaluated conformations by CD. We found that changes in pH corresponded to changes in conformation. This led us to conclude that pH causes a completely reversible equilibrium denaturation of 3βHSD2. The pH-mediated changes in CD and fluorescence spectra of the protein may be described reasonably well by a simple three-state denaturation/renaturation model. However, the chaotropic agent GdmHCl induced further denaturation of the same protein, which indicates the presence of a stable folding intermediate that represents a significant portion of the equilibrium population. This intermediate retains a significant amount of secondary structure, amounting to ~30% of the native protein. The folding intermediate observed after incubation with GdmHCl was not due to differential denaturation of monomeric and dimeric 3βHSD2, because the denaturation profile and CD spectra of 3βHSD2 over a 50-fold range in concentration clearly showed that the protein is monomeric.

Several scenarios could account for the presence of a stable intermediate after denaturation of 3βHSD2. The simplest explanation is that GdmHCl only partially denatures the protein, with the first transition producing the observed metastable intermediate. Even after incubation in 2 M GdmHCl, there may be some residual secondary structure remaining at pH 7.4. When we decreased the pH, it appeared that this metastable state persisted until pH 5.5. With a further decrease in pH, although, the metastable state underwent a two-step cooperative unfolding due to the presence of additional hydrogen ions.

A second scenario is that GdmHCl stabilizes an intermediate, increasing its equilibrium concentration. If nondenaturing concentrations of GdmHCl stabilize a folding intermediate, relatively low concentrations of GdmHCl might also lead to accumulations of the intermediate similar to acid-induced denaturation. Incubating nondenaturing concentrations of GdmHCl (0.5–1.14 M) with protein at pH 5.5 resulted in a directly biphasic denaturation (Fig. 6*A*), reminiscent of what we observed with GdmHCl-induced denaturation. Based on the ellipticity at 222 nm, we calculated the free energy, and then plotted these values as a function of the GdmHCl concentra-

tion. Through extrapolation, we determined that the ΔG_0 value in the absence of denaturant equaled 1.9 kcal/mol and used this as an independent estimate of the free energy of the N ⇔ *I* transition. This value is similar to that observed in the absence of acid denaturation. The second transition, $I_{1I} \rightarrow$ U, is more difficult to quantitate because it occurs at higher denaturant concentrations and produces a somewhat smaller signal change; however, it appears that increasing the GdmHCl concentration increases the free energy difference between the intermediate and unfolded state. With increasing acid denaturation in the presence of GdmHCl, the sum of the free energy change for the N ⇔ I_I and I_{1I} ⇔ U transitions is nearly constant at 1.3 kcal/mol, particularly at the intermediate concentrations of GdmHCl as these concentrations yield the most accurate ΔG measurements. This suggests that the estimated free energy difference between native and unfolded states is independent of the concentration of GdmHCl and that the accumulation of the intermediates results from GdmHCl-mediated stabilization. Thus, there appears to be an equilibrium between I_I to I_{1I}. Maintaining an equilibrium state would conserve energy, resulting in a stable protein that can revert back to its native conformation when the pH reaches 7.4.

The fact that denaturation by pH in the absence of GdmHCl is characterized by a $\Delta G_{N \rightarrow U}$ of 0.78 kcal/mol rather than 1.9 kcal/mol and the observation that the residue ellipticity pH 3.5 is significantly higher than that at 6 M GdmHCl implies that denaturation in pH alone produces a less stable intermediate that is difficult to detect experimentally. If our model is correct and the $\Delta G_{N \rightarrow U}$ is independent of the denaturant, then we would expect ΔG from $I_I \rightarrow I_{II}$ would have a value of ~0.5 kcal. Thus, the inferred stability of the intermediate in the absence of GdmHCl is consistent with the inability to observe it initially.

Based on this data, we have concluded that 3βHSD2 is in a molten globule state at the IMM, which promotes activity. Folding can (34) proceed through a variety of intermediate states with decreasing Gibbs free energies (35). The intermediates may comprise partially folded forms of individual domains or of the entire protein: intermediates that have attained a high degree of secondary structure but lack defined tertiary structure are often termed "molten globules" (36). Molten globules can be viewed as highly dynamic, collapsed, compact polypeptide chains maintained by hydrophobic interactions that promote helical conformations but that lack fixed, specific long-range interactions (37–40). Studies with bacterial β-barrel proteins have shown that insertion into the mitochondrial membrane causes the proteins to form molten-disc intermediates that have a partial secondary structure with the β-strands sitting flat on the membrane surface (11). This likely occurs in eukaryotic mitochondrial proteins as the membrane insertion pathway is fairly conserved (41). Molten globules are incompletely folded proteins and may go through molten globule intermediate states during membrane insertion (42) and biological activity is highly questionable at the molten globule state. However, in the present study the 3βHSD2 is 7-fold more active at pH 4.5 than the protein in its native state, pH 7.4. This observation is further supported by the higher efficiency of ANS binding to the molten globule conformation of 3βHSD2 at around pH 4.5 (31).

We also did stopped-flow spectrophotometry to measure real time unfolding of 3βHSD2, and found the results consistent with a molten globule conformation. The protein rate of unfolding was observed only when the outer hydrophobic core was opened at or below pH 3.25 followed by relaxation. Also, the rate of unfolding between pH 4 and 5 embedding of the burst phase with the relaxation time, which is the condition of partial opening and existence of the molten globule conformation.

3βHSD2 has an overall very flexible conformation (43). We had previously shown that the protein has no defined protease-resistant domain (3). The N-terminal mitochondrial leader sequence is the most hydrophobic portion of 3βHSD2, and secondary structure predictions suggest that all regions of the protein are highly structured, but flexible due to the presence of the Rossmann-fold domain, with a β-α-β-α-β-α-β-α-β-α-β folding pattern that binds cofactor and substrate (44). An electrostatic interaction could occur between the positively charged residues of 3βHSD2 and the negatively charged cofactors, resulting in a molten-disc conformation (11). The additional ejected protons in the IMS are likely to be absorbed by the lipid vesicles (45). Alternatively, small structured domains of 3βHSD2 might interact with an as yet unidentified receptor on the IMM or at the IMS. In either event, the physical data suggest that the helices in the soluble active 3βHSD2 structure could be preserved in the IMM (42), suggesting that the membrane bound protein retains its flexible conformation.

Enzymes catalyzing proton transfer are arranged asymmetrically on the inner mitochondrial membrane so that protons are transferred across the two-mitochondrial membranes. This proton pump establishes an electrochemical gradient leading to a local reduction of pH inside the mitochondria. If the interaction of 3βHSD2 with the inner mitochondrial membrane causes a reduction in the membrane potential ($\Delta\Psi$) (42), our data suggest that this would increase the flexibility of the N-terminal hydrophobic region by accepting or releasing the additional hydrogen ions. Thus partial unfolding induced by the mitochondrial electrochemical gradient and by inner mitochondrial compartmental location would result in the transition to a molten globule state (11, 46). By preserving some secondary structure, the molten globule state would provide the best pathway for minimizing the energetic cost and also the most active form for the catalysis of pregnenolone to progesterone. This will allow 3βHSD2 to interact directly with the outer and inner mitochondrial translocase at the inter membrane space (3), as this transition to a flexible conformation lowers the energy required to open the structure, possibly supporting the ability to participate in two different steps as described by our model.

Acknowledgments—Funding for equipment in the Mass Spectrometry Facility at the University of Alberta is supported by the Canada Foundation for Innovation and Alberta Science and Research Investment Program.

REFERENCES

1. Rhéaume, E., Lachance, Y., Zhao, H. F., Breton, N., Dumont, M., de Launoit, Y., Trudel, C., Luu-The, V., Simard, J., and Labrie, F. (1991) Structure and expression of a new complementary DNA encoding the almost exclusive 3β-hydroxysteroid dehydrogenase/δ5-δ4-isomerase in human adrenals and gonads. *Mol. Endocrinol.* **5,** 1147–1157

2. Persson, B., Kallberg, Y., Bray, J. E., Bruford, E., Dellaporta, S. L., Favia, A. D., Duarte, R. G., Jörnvall, H., Kavanagh, K. L., Kedishvili, N., Kisiela, M., Maser, E., Mindnich, R., Orchard, S., Penning, T. M., Thornton, J. M., Adamski, J., and Oppermann, U. (2009) The SDR (short chain dehydrogenase/reductase and related enzymes) nomenclature initiative. *Chem. Biol. Interact.* **178,** 94–98
3. Pawlak, K. J., Prasad, M., Thomas, J. L., Whittal, R. M., and Bose, H. S. (2011) Inner mitochondrial translocase Tim50 interacts with 3β-hydroxysteroid dehydrogenase type 2 to regulate adrenal and gonadal steroidogenesis. *J. Biol. Chem.* **286,** 39130–39140
4. Truscott, K. N., Brandner, K., and Pfanner, N. (2003) Mechanisms of protein import into mitochondria. *Curr. Biol.* **13,** R326–337
5. Jensen, R. E., and Johnson, A. E. (2001) Opening the door to mitochondrial protein import. *Nat. Struct. Biol.* **8,** 1008–1010
6. Glick, B. S., Brandt, A., Cunningham, K., Muller, S., Hallberg, R. L., and Schatz, G. (1992) Cytochromes c1 and b2 are sorted to the intermembrane space of yeast mitochondria by a stop-transfer mechanism. *Cell* **69,** 347–357
7. Levy, Y., Cho, S. S., Onuchic, J. N., and Wolynes, P. G. (2005) A survey of flexible protein binding mechanisms and their transition states using native topology based energy landscapes. *J. Mol. Biol.* **346,** 1121–1145
8. Sali, A., Shakhnovich, E., and Karplus, M. (1994) How does a protein fold? *Nature* **369,** 248–251
9. Onuchic, J. N., and Wolynes, P. G. (2004) Theory of protein folding. *Curr. Opin. Struct. Biol.* **14,** 70–75
10. Onuchic, J. N., Luthey-Schulten, Z., and Wolynes, P. G. (1997) Theory of protein folding. The energy landscape perspective. *Annu. Rev. Phys. Chem.* **48,** 545–600
11. Tamm, L. K., Hong, H., and Liang, B. (2004) Folding and assembly of β-barrel membrane proteins. *Biochim. Biophys. Acta* **1666,** 250–263
12. Miller, W. L., and Auchus, R. J. (2011) The molecular biology, biochemistry, and physiology of human steroidogenesis and its disorders. *Endocr. Rev.* **32,** 81–151
13. Thomas, J. L., Myers, R. P., and Strickler, R. C. (1989) Human placental 3 beta-hydroxy-5-ene-steroid dehydrogenase and steroid 5–4-ene-isomerase: purification from mitochondria and kinetic profiles, biophysical characterization of the purified mitochondrial and microsomal enzymes. *Steroid Biochem.* **33,** 209–217
14. Thomas, J. L., Mason, J. I., Brandt, S., Spencer, B. R., Jr., and Norris, W. (2002) Structure/function relationships responsible for the kinetic differences between human type 1 and type 2 3β-hydroxysteroid dehydrogenase and for the catalysis of the type 1 activity. *J. Biol. Chem.* **277,** 42795–42801
15. Gill, S. C., and von Hippel, P. H. (1989) Calculation of protein extinction coefficients from amino acid sequence data. *Anal. Biochem.* **182,** 319–326
16. Bose, M., Debnath, D., Chen, Y., and Bose, H. S. (2007) Folding, activity, and import of steroidogenic acute regulatory protein into mitochondria changed by nicotine exposure. *J. Mol. Endocrinol.* **39,** 67–79
17. Bose, M., Whittal, R. M., Miller, W. L., and Bose, H. S. (2008) Steroidogenic activity of StAR requires contact with mitochondrial VDAC1 and phosphate carrier protein. *J. Biol. Chem.* **283,** 8837–8845
18. Sreerama, N., Venyaminov, S. Y., and Woody, R. W. (2000) Estimation of protein secondary structure from circular dichroism spectra. Inclusion of denatured proteins with native proteins in the analysis. *Anal. Biochem.* **287,** 243–251
19. Sreerama, N., and Woody, R. W. (1993) A self-consistent method for the analysis of protein secondary structure from circular dichroism. *Anal. Biochem.* **209,** 32–44
20. Sreerama, N., and Woody, R. W. (2000) Estimation of protein secondary structure from circular dichroism spectra: comparison of CONTIN, SELCON, and CDSSTR methods with an expanded reference set. *Anal. Biochem.* **282,** 252–260
21. Sreerama, N., and Woody, R. W. (2004) Computation and analysis of protein circular dichroism spectra. *Methods Enzymol.* **383,** 318–351
22. Ali, V., Kulkarni, P. K., Ahmad, A., Madhusudan, K. P., and Bhakuni, V. (1999) 8-anilino-1-naphthalene sulfonic acid (ANS) induces folding of acid unfolded cytochrome c to molten globule state as a result of electrostatic interactions. *Biochemistry* **39,** 13635–13642
23. Wang, J. L., and Edelman, G. M. (1971) Fluorescent probes for conformational states of proteins. IV. The pepsinogen-pepsin conversion. *J. Biol. Chem.* **246,** 1185–1191
24. Akiyama, S., Takahashi, S., Ishimori, K., and Morishima, I. (2000) Stepwise formation of alpha-helices during cytochrome c folding. *Nat. Struct. Mol. Biol.* **7,** 514–520
25. Schleyer, M., and Neupert, W. (1985) Transport of proteins into mitochondria. Translocational intermediates spanning contact sites between outer and inner membranes. *Cell* **43,** 339–350
26. Pfanner, N., Tropschug, M., and Neupert, W. (1987) Mitochondrial protein import. Nucleoside triphosphates are involved in conferring import-competence to precursors. *Cell* **49,** 815–823
27. Chen, W. J., and Douglas, M. G. (1987) Phosphodiester bond cleavage outside mitochondria is required for the completion of protein import into the mitochondrial matrix. *Cell* **49,** 651–698
28. Fasman, G. D. (ed) (1996) *Circular Dichroism and the Conformational Analysis of Biomolecules*, Plenum Press, New York
29. Woody, R. W., and Dunker, A. K. (1996) in *Circular Dichroism and Conformational Analysis of Biomolecules* (Fasman, G. D., ed) pp. 109–144, Plenum Press, New York
30. Semisotnov, G. V., Rodionova, N. A., Razgulyaev, O. I., Uversky, V. N., Gripas', A. F., and Gilmanshin, R. I. (1991) Study of the "molten globule" intermediate state in protein folding by a hydrophobic fluorescent probe. *Biopolymers* **31,** 119–128
31. Cunningham, E. L., and Agard, D. A. (2003) Interdependent folding of the N- and C-terminal domains defines the cooperative folding of α-lytic protease. *Biochemistry* **42,** 13212–13219
32. Huang, C. Y. (1982) Determination of binding stoichiometry by the continuous variation method: the Job plot. *Methods Enzymol.* **87,** 525–529
33. Agashe, V. R., Shastry, M. C., and Udgaonkar, J. B. (1995) Initial hydrophobic collapse in the folding of barstar. *Nature* **377,** 754–757
34. Redfield, C., Smith, L. J., Boyd, J., Lawrence, G. M., Edwards, R. G., Gershater, C. J., Smith, R. A., and Dobson, C. M. (1994) Analysis of the solution structure of human interleukin-4 determined by heteronuclear three-dimensional nuclear magnetic resonance techniques. *J. Mol. Biol.* **238,** 23–41
35. Brooks, C. L., 3rd, Gruebele, M., Onuchic, J. N., and Wolynes, P. G. (1998) Chemical physics of protein folding. *Proc. Natl. Acad. Sci. U.S.A.* **95,** 11037–11038
36. Privalov, P. L. (1996) Intermediate states in protein folding. *J. Mol. Biol.* **258,** 707–725
37. Kuwajima, K. (1989) The molten globule state as a clue for understanding the folding and cooperativity of globular-protein structure. *Proteins Struct. Funct Genet.* **6,** 87–103
38. Kuwajima, K., Garvey, E. P., Finn, B. E., Matthews, C. R., and Sugai, S. (1991) Transient intermediates in the folding of dihydrofolate reductase as detected by far-ultraviolet circular dichroism spectroscopy. *Biochemistry* **30,** 7693–7703
39. Chan, H. S., and Dill, K. A. (1991) Polymer principles in protein structure and stability. *Annu. Rev. Biophys. Biophys. Chem.* **20,** 447–490
40. Ptitsyn, O. (1995) Molten globule and protein folding. *Adv. Protein Chem.* **47,** 83–229
41. Walther, D. M., Papic, D., Bos, M. P., Tommassen, J., and Rapaport, D. (2009) Signals in bacterial β-barrel proteins are functional in eukaryotic cells for targeting to and assembly in mitochondria. *Proc. Natl. Acad. Sci. U.S.A.* **106,** 2531–2536
42. van der Goot, F. G., González-Mañas, J. M., Lakey, J. H., and Pattus, F. (1991) A "molten-globule" membrane-insertion intermediate of the pore-forming domain of colicin A. *Nature* **354,** 408–410
43. Thomas, J. L., Duax, W. L., Addlagatta, A., Brandt, S., Fuller, R. R., and Norris, W. (2003) Structure/function relationships responsible for coenzyme specificity and the isomerase activity of human type 1 3β-hydroxysteroid dehydrogenase/isomerase. *J. Biol. Chem.* **278,** 35483–35490
44. Jörnvall, H., Persson, B., Krook, M., Atrian, S., Gonzàlez-Duarte, R., Jeffery, J., and Ghosh, D. (1995) Short chain dehydrogenases/reductases (SDR). *Biochemistry* **34,** 6003–6013
45. Rajapaksha, M., Thomas, J. L., Streeter, M., Prasad, M., Whittal, R. M., Bell, J. D., and Bose, H. S. (2011) Lipid-mediated unfolding of 3β-hydroxysteroid dehydrogenase 2 is essential for steroidogenic activity. *Biochemistry* **50,** 11015–11024
46. Ryan, K. R., and Jensen, R. E. (1995) Protein translocation across mitochondrial membranes. What a long, strange trip it is. *Cell* **83,** 517–519